View metadata, citation and similar papers at core.ac.uk
brought to you by CORE

ISSN 1063-7826, Semiconductors, 2007, Vol. 41, No. 8, pp. 973–978. © Pleiades Publishing, Ltd., 2007.
Original Russian Text © V.B. Zalesski, V.Yu. Rud', V.F. Gremenok, Yu.V. Rud', T.R. Leonova, A.V. Kravchenko, E.P. Zaretskaya, M.S. Tivanov, 2007, published in Fizika i Tekhnika Poluprovodnikov, 2007, Vol. 41, No. 8, pp. 992–997.

PHYSICS OF SEMICONDUCTOR DEVICES

Cadmium-free Thin-Film $Cu(In,Ga)Se_2/(In_2S_3)$ Heterophotoelements: Fabrication and Properties

V. B. Zalesski[a], V. Yu. Rud'[b]^, V. F. Gremenok[c], Yu. V. Rud'[d], T. R. Leonova[a], A. V. Kravchenko[a], E. P. Zaretskaya[c], and M. S. Tivanov[c]

[a]*Institute of Electronics, National Academy of Sciences of Belarus, Minsk, 220090 Belarus*
[b]*St. Petersburg State Polytechnical University, St. Petersburg, 195251 Russia*
^*e-mail: rudvas@spbstu.ru*
[c]*Joint Institute of Solid-State and Semiconductor Physics, National Academy of Sciences of Belarus, Minsk, 220072 Belarus*
[d]*Ioffe Physicotechnical Institute, Russian Academy of Sciences, St. Petersburg, 194021 Russia*

Submitted November 29, 2006; accepted for publication December 15, 2006

Abstract—The method of heat treatment of metallic Cu–In–Ga layers in the N_2 inert atmosphere in the presence of selenium and sulfur vapors was used to grow homogeneous films of $Cu(In,Ga)(S,Se)_2$ alloys onto which the CdS or In_2S_3 films were deposited and, on the basis of these structures, the thin-film glass/Mo/*p*-Cu(In,Ga)$(S,Se)_2$/*n*-(In_2S_3,CdS)/*n*-ZnO/Ni–Al photoelements were fabricated. The mechanisms of charge transport and the processes of photosensitivity in the obtained structures subjected to irradiation with natural and linearly polarized light are discussed. The broadband photosensitivity of thin-film heterophotoelements and the induced photopleochroism were detected; these findings indicate that there is an interference-related blooming of the structures obtained. It is concluded that it is possible to use ecologically safe cadmium-free thin-film heterostructures as high-efficiency photoconverters of solar radiation.

PACS: 78.20.-e, 81.15.-z, 85.30.Hi
DOI: 10.1134/S1063782607080210

1. INTRODUCTION

Basic studies of diamond-like semiconductor compounds in the direction of complicating their atomic composition have given rise to considerable progress in the physics and technology of semiconductors and led, in particular, to the fabrication of experimental thin-film heterophotoelemenrs (TFHPs) glass/Mo/Cu(In,Ga)Se_2/CdS/ZnO/Ni–Al with unprecedentedly high quantum efficiency (~19.8%) and extraordinary radiation resistance [1-4]. However, the complexity of the method of simultaneous vacuum evaporation of all components of the Cu(In,Ga)Se_2 (CuInGaSe) solid solution and the high toxicity of the components (H_2Se and CdS) used in the fabrication of TFHPs still impose restrictions on the already long-standing necessity of commercial production of these solar cells [3, 5, 6]. An alternative technology for the production of thin-film (~2 μm) CuInGaSe with the composition required for efficient conversion of solar energy to electricity is based on the heat treatment of the base Cu–In–Ga layers in Se vapors that appear in the reaction zone with the H_2Se gas flow, which restricts the use of this technology in the mass production of photoconverters [6]. At present, the time has come to start the active search for commercial ecologically safe technologies for growing large-area CuInGaSe films and obtaining the TFHPs on the basis of these films. This study is a continuation of the important line of research in modern photoenergy engineering and is concerned with development of the technology of cadmium-free Cu(In,Ga)Se_2/In_2S_3 TFHPs; we also study for the first time the properties of these TFHPs and compare them with those of conventional photoconverters based on Cu(In,Ga)$(S,Se)_2$/CdS.

2. RESULTS AND DISCUSSION

2.1. Homogeneous CuInGaSe films were obtained using heat treatment of the starting Cu–In–Ga layers with the component composition necessary for the synthesis of the required solid solution. The Cu–In–Ga films were deposited using ion-plasma evaporation of the target of these metals in vacuum ($\sim 6 \times 10^{-4}$ Pa) onto glass substrates (either with a specially prepared surface or with a molybdenum sublayer) heated to 100°C. Heat treatment of the initial Cu–In–Ga films was carried out in the nitrogen inert atmosphere in the presence of selenium vapors in the temperature range of 250–520°C. Physicochemical studies showed that these conditions of heat treatment ensured the synthesis of a quaternary solid solution with chalcopyrite structure [7]. The duration of the process was chosen so as to satisfy the conditions for completion of the reaction of forma-

Table 1. Atomic composition of the $Cu(In,Ga)Se_2$ and $Cu(In,Ga)(S,Se)_2$ films obtained using heat treatment of the Cu–In–Ga layers in the atmosphere of Se, S, and N_2

Sample no.	Atomic composition, at %				
	Cu	In	Ga	Se	S
1MX178S	28.14	22.37	4.24	36.68	8.57
1MX200	27.55	23.36	1.37	47.72	–

tion of homogeneous films of quaternary solid solution with the required composition.

Studies of the films by the method of X-ray analysis using the CuK_α radiation and a Ni filter showed that the developed technology results in the formation of an equilibrium alloy with a chalcopyrite lattice whose parameters are consistent with Vegard's rule.

An analysis of the elemental composition of the grown films was performed using a PHI-660 scanning Auger microscope with spatial resolution of ~0.1 μm and sensitivity of ~0.1 at %. The results of these studies for typical films are listed in Table 1. It is worth noting that the obtained CuInGaSe films were highly homogeneous over the surface.

The combination of the performed studies of homogeneous p-$Cu(In,Ga)Se_2$ films also indicated that it is possible to control the atomic composition and distribution of the component over the cross section [7]. The concentration of free holes at $T = 300$ K in the films under consideration was $\sim 2 \times 10^{18}$ cm^{-3} and the hole mobility was about 70 cm^2 V^{-1} s^{-1}.

In order to obtain a TFHP, we used the method of vacuum thermal evaporation to deposit In_2S_3 films with the thickness of ~40 nm onto the outer surface of the p-CuInGaSe films [8]. The method of magnetron sputtering was used to deposit first a high-resistivity ZnO film ($d_l \approx 20$–40 nm, $\rho \approx 2.0 \times 10^7$ Ω cm) onto the surface of these films, followed by an aluminum-doped low-resistivity n-ZnO film ($d_l \approx 0.5$ nm, $\rho = 3 \times 10^{-3}$–3×10^{-4} Ω cm, $\mu = 18$ cm^2 V^{-1} s^{-1}, and $n = 1.4 \times 10^{20}$ cm^{-3} at $T = 300$ K). To conclude the process, we used the method of vacuum thermal evaporation through a mask to form Ni–Al current contacts on the surface of the n-ZnO film.

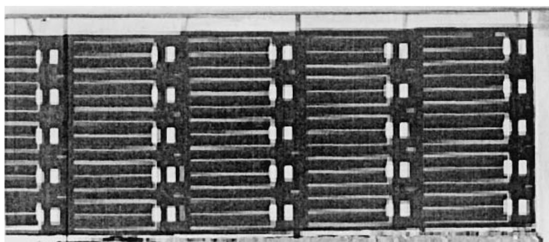

Fig. 1. External appearance of a thin-film glass/Mo/p-$Cu(In,Ga)Se_2$/n-In_2S_3/n-ZnO/Ni–Al heterophotoelements on the substrate with dimensions 25 × 75 mm.

The thin-film glass/Mo/p-Cu(In,Ga)Se_2/In_2S_3/ZnO/Ni–AL photoconverters were formed on the substrates with the dimensions ~2 × 25 × 75 mm; the method of mechanical scribing was then used to form a number of elements with the area of ~5 × 10 mm^2, each of which was provided with a current contact; the Mo film with the thickness of 0.5–0.8 μm deposited on the glass served as the common contact for all TFHPs. In Fig. 1, we show the external view of this photoelement.

We also obtained the glass/p-Cu(In,Ga)(S,Se)$_2$/CdS/n-ZnO/Ni–Al TFHPs in a similar way. The sulfur concentration in the p-$Cu(In,Ga)(S,Se)_2$ (CuInGaSSe) films was governed by the parameters of the sulfidizing process and is listed in Table 1. The barrier n-CdS films with the thickness of 40–50 nm were deposited onto the CuInGaSSe surface using the chemical method [9].

2.2. Studies of the static current-voltage (I–V) characteristics showed that the obtained Mo/p-CuInGaSe/n-In_2S_3 TFHPs exhibit pronounced rectification with the conducting direction always observed at the negative polarity of external bias applied to the n-In_2S_3 film. The rectification factor in the obtained TFHPs was $K \approx 3$–25 at the bias voltages $|U| \approx 1$ V. A typical I–V characteristic of one of the CuInGaSe/In_2S_3 elements is shown in Fig. 2. The initial portion of the forward I–V characteristic ($U < 0.5$ V) for these structures is consistent with the well-known diode equation (Fig. 2b, curve *1*) with the diode factor $\beta \approx 1.93$ (Table 2). This value of β indicates that the forward current is caused by recombination of charge carriers in the active region of these TFHPs. At the same time, for the CuInGaSSe/CdS TFHP, we have $\beta \approx 4.25$ (Table 2), which is much larger than in the case of the CuInGaSe/In_2S_3 barriers. This circumstance is typically related to variations in the charge transport due to a decrease in the structural quality of the heterointerface and indicates that the forward current is governed by the tunnel-recombination mechanism [10].

At the forward-bias voltages $U > 0.5$ V (Fig. 2a), the I–V characteristic of the structures based on In_2S_3 and CdS starts to be linear,

$$I = \frac{U - U_0}{R_0}, \qquad (1)$$

where the cutoff voltage $U_0 = 0.3$–04 V (Table 2), while the residual resistance R_0 for various structures varies in the range from 100 to 200 Ω at $T = 300$ K.

The reverse portions of the I–V characteristics of the compared types of TFHPs are typically described by the power-law dependence $|I| \propto |U|^m$, where the exponent m is found to be close to unity at $|U| \lesssim 0.3$ V

(Fig. 2c), which may indicate that there is tunneling of charge carriers or limitation of the current by the space charge in the saturation mode [11]. As the magnitude of the reverse-bias voltage is increased ($|U| > 0.4$ V), the exponent attains a value of $m \approx 1.6$, which is consistent with the Childe–Langmuir law and is typically related to the currents limited by the space charge in the ballistic mode [12, 13].

Thus, the replacement of the CdS barrier layer by the In_2S_3 layer in the obtained TFHPs does not bring about significant changes in their electrical properties but ensures the elimination of highly toxic cadmium from their composition.

2.3. The photovoltaic effect caused by separation of photogenerated charge-carrier pairs in the active region of the CuInGaSe/In_2S_3 structures is clearly and reproducibly observed in the TFHPs based on the CuInGaSe films grown by selenization of the base Cu–In–Ga layers in the N_2 atmosphere and subjected to illumination. The dependence of the open-circuit photovoltage U_{oc} and the short-circuit current J_{sc}, in accordance with [10], on the optical-flux power, is described by the logarithmic and linear laws, respectively. In Table 2, we list the values of J_{sc} and the saturation photovoltage U_∞ of typical TFHPs with the In_2S_3 and CdS barriers. It can be seen that, at the incident-radiation power $L \approx$ 100 mW/cm^2, the maximum value $J_{sc}^m \approx 35$ mA/cm^2 is attained in a TFHP with the CuInGaSSe/In_2S_3 active region, which is close to the similar parameter in the conventionally used active region of the CuInGaSSe/CdS structure (Table 2). A similar situation for the TFHPs to be compared is also observed in relation to U_∞ (Table 2) close to the cutoff voltage U_0 in the same structures and can be identified with the energy-barrier height that was found to be almost identical for the used barrier materials (CdS and In_2S_3).

It is worth noting that, in the TFHPs based on CuInGaSe films and obtained by selenization, the saturation photovoltage U_∞ was found to be almost two times lower than that for TFHPs based on thin films with similar composition and grown by coevaporation of the alloy's components [3, 13]. At the same time, an analysis of Table 2 makes it possible to conclude that a higher quantum efficiency of photoconversion is attained if the barriers from In_2S_3 films are used in TFHPs based on CuInGaSe layers.

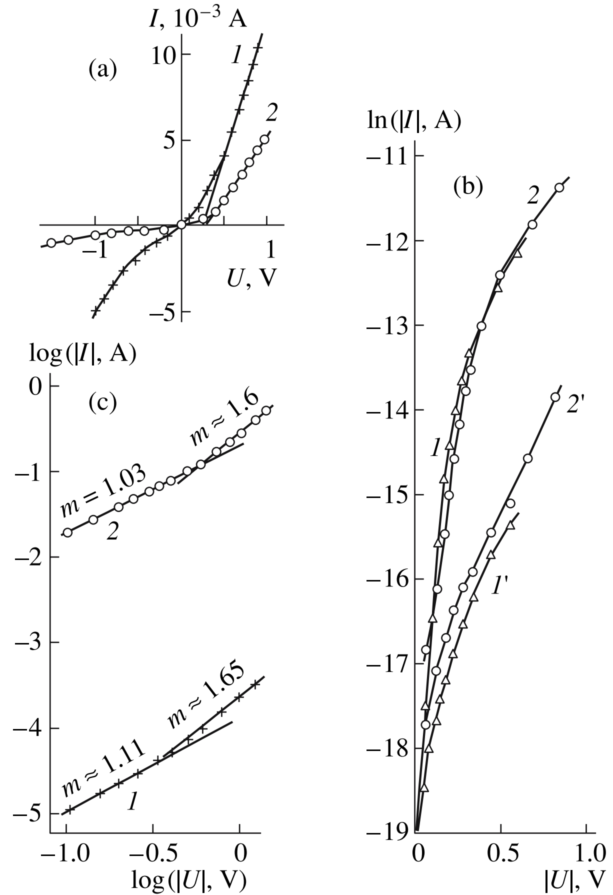

Fig. 2. Static current-voltage characteristics (T = 300 K) of the heterophotoelements glass/Mo/p-Cu(In,Ga)Se_2/n-In_2S_3/n-ZnO/Ni–Al (sample 1MX201-2, curves *1* and *1'*) and glass/Mo/p-Cu(In,Ga)(S,Se)$_2$/n-CdS//n-ZnO/Ni–Al (sample 1MX178S, curves *2* and *2'*) in the representations (a) $I = f(U)$, (b) $\ln|I| = f(U)$, and (c) $\log|I| = f(\log U)$.

2.4. In Fig. 3, we show typical spectra of relative quantum efficiency of photoconversion $\eta(\hbar\omega)$ for TFHPs obtained by deposition of the barrier films of In_2S_3 (curves *1*, *1'*) and CdS (curves *2*, *2'*) onto the surface of the films Cu(In,Ga)Se_2 and Cu(In, Ga)(S, Se)$_2$, respectively. It can be seen that a high photosensitivity is observed in a wide spectral range from 1 to 3.8 eV.

Table 2. Photoelectric properties of thin-film Cu(In,Ga)(S,Se)$_2$/CdS(In_2S_3) heterophotoelements at T = 300 K

Sample no.	Type of the structure	β	R_0, Ω	U_0, V	K (U = 1 V)	J_{sc}^m, mA/cm^2	U_∞, V	η, %	$\hbar\omega^m$, eV	$\delta_{1/2}$, eV	S_U^m, V/W	E_G^d, eV	P_I, % (Θ ≈ 70°, $\hbar\omega \approx 1.5$ eV)
1MX178S	CIGSSe/CdS	4.25	125	0.30	12	24	0.35	2.4	1.6–1.8	1.9	25	1.06	12
1MX187	CIGSe/In_2S_3	–	94	0.26	3	29	0.25	3.2	1.2–1.7	1.8	15	0.98	5
1MX200	CIGSe/In_2S_3	–	200	0.40	12	28	0.33	3.9	1.2–2.1	1.95	125	0.95	4
1MX201-2	CIGSe/In_2S_3	1.93	170	0.38	25	35	0.38	4.7	1.3–1.9	1.95	400	0.95	7

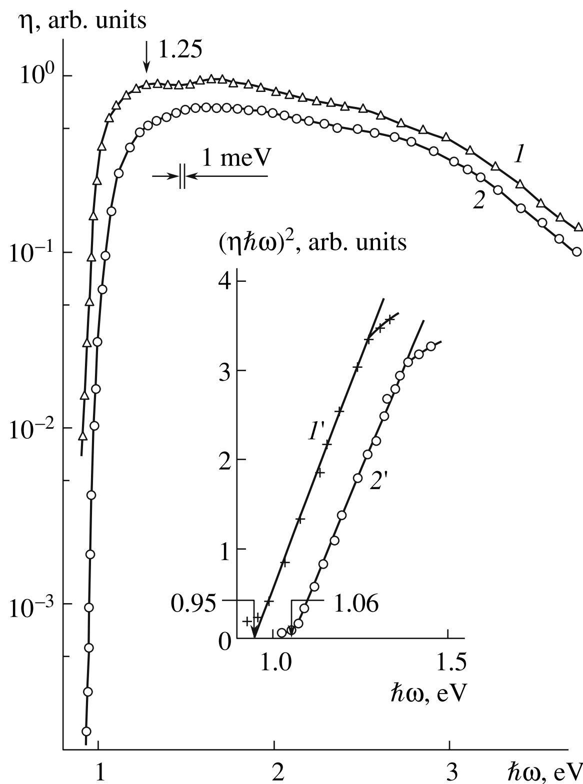

Fig. 3. Spectra of relative quantum efficiency of photoconversion η (curves *1*, *2*) and dependences $(\eta\hbar\omega)^2 = f(\hbar\omega)$ (curves *1*', *2*') for heterophotoelements glass/Mo/*p*-Cu(In, Ga)Se_2/*n*-In_2S_3/*n*-ZnO/Ni–Al (sample 1MX201-2, curves *1*, *1*') and glass/Mo/*p*-Cu(In,Ga)(S,Se)$_2$/*n*-CdS/*n*-ZnO/Ni–Al (sample 1MX178S, curves *2*, *2*') irradiated with nonpolarized light. The *n*-ZnO side of the structure was illuminated. $T = 300$ K. Curves *1* and *2* are shifted along the vertical axis.

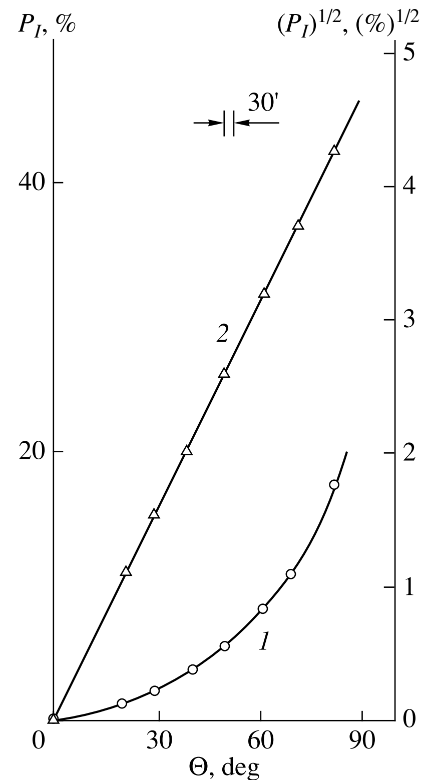

Fig. 4. Dependences of the coefficient of induced photopleochroism P_I (curve *1*) and $P_I^{1/2}$ (curve *2*) at $T = 300$ K on the angle of incidence Θ of linearly polarized light onto the receiving plane of the heterophotoelement glass/Mo/*p*-Cu(In,Ga)Se_2/*n*-In_2S_3/*n*-ZnO/Ni–Al (sample 1MX201-2, $\hbar\omega = 2$ eV).

A steep long-wavelength rise of photosensitivity is observed at $\hbar\omega > 0.95$ eV (Fig. 3, curves *1*, *2*). For both types of barriers, the dependences $\eta(\hbar\omega)$ are linearized in the representation $(\eta\hbar\omega)^2 = f(\hbar\omega)$ (Fig. 3, curves *1*', *2*'). The extrapolation $(\eta\hbar\omega)^2 \longrightarrow 0$ on the basis of the theory of interband absorption in semiconductors [10] made it possible to determine the band gap for direct interband transitions E_G^d (Table 2); the value of E_G is in satisfactory agreement with the corresponding estimates based on the data on optical transmission of the same films. It is noteworthy that the spectral contour $\eta(\hbar\omega)$ and the value of E_G^d determined from the measurements of photosensitivity of the barriers under study were found to be quite reproducible over the entire area of the films. This finding is also consistent with the electron-microscopy data on the high local homogeneity of the films grown in the processes of selenization and sulfurization of metallic Cu–In–Ga layers.

It also follows from Fig. 3 (curves *1*, *2*) that, as the energy of incident photons is increased ($\hbar\omega > E_G^d$), the photosensitivity continues to increase in the spectra $\eta(\hbar\omega)$ for photoelements based on different barrier materials (CdS and In_2S_3); the photosensitivity η starts to gradually decrease only at $\hbar\omega > 1.6$ eV. As a result, the total width of the $\eta(\hbar\omega)$ spectra at their half-height for the best structures based on the In_2S_3 and CdS films was found to be as large as $\delta_{1/2} \approx 1.95$ eV for both types of structures (Table 2). This finding indicates that the quality of the interface is fairly high and is not worsened as a result of replacement CdS $\longrightarrow$ In_2S_3, which is also corroborated by the close values of photocurrent J_{sc} in the TFHPs under comparison (Table 2). The highest voltage sensitivity $S_U^m \approx 400$ V/W is observed for a TFHP based on the CuInGaSe/In_2S_3 barrier; the highest quantum efficiency is also characteristic of this TFHP (Table 2).

2.5. Using irradiation of TFHPs with linearly polarized light (LPL), Rud' et al. [13–15] established that there is no natural photopleochroism in these photoelements. This feature is related to the fact that all layers of these TFHPs are polycrystalline. Under conditions

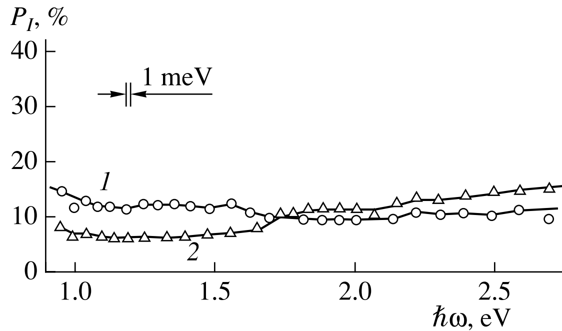

Fig. 5. Spectra $P_I(\hbar\omega)$ of heterophotoelements glass/Mo/*p*-Cu(In,Ga)Se_2/*n*-In_2S_3/*n*-ZnO/Ni–Al (sample 1MX201-2, curve *1*) and glass/Mo/*p*-Cu(In, Ga)(S,Se)$_2$/CdS/*n*-ZnO/Ni–Al (sample 1MX178S, curve *2*) at $T = 300$ K.

of oblique incidence of LPL on the receiving ZnO plane, as soon as the angle of incidence Θ becomes nonzero, the TFHP starts to exhibit induced photopleochroism $P_I > 0$ [15]. In Fig. 4, we show the typical dependence of the induced-photopleochroism coefficient on the angle of incidence of LPL. It follows from Fig. 4 that this dependence is consistent with the theory and is described by the square law [14, 15]

$$P_I \propto \Theta^2 \qquad (2)$$

for both types of TFHPs (curves *1*, *2*). However, the coefficient of induced photopleochroism was found to be much smaller than the value estimated from the theory $P_I \approx 30\%$, with rgw refractive index of ZnO taken into account [15, 16].

Typical $P_I(\hbar\omega)$ spectra at a fixed angle of the LPL incidence $\Theta = 70°$ for TFHPs with the In_2S_3 and CdS barrier forms are shown in Fig. 5. It can be seen that the coefficient of induced photopleochroism depends only slightly on the photon energy and is extremely small in the entire range of photosensitivity. The value of this coefficient is about two times smaller than what is expected from the theory [15]. We can state that the established trends of induced photopleochroism in the obtained TFHPs are indicative of the effect of interference-related bleaching of these photoelements in the entire spectral range of photoconversion as a result of deposition of thin ZnO films onto the outer plane of the CdS and In_2S_3 barrier layers [14, 15]. Evidently, the optimization of magnetron-assisted deposition of ZnO films would make it possible to increase the quantum efficiency of photoconversion in a TFHP, while the use of polarization photoelectric spectroscopy ensures the rapid monitoring of the processes of formation of antireflection single-layer coatings from thin ZnO films.

3. CONCLUSIONS

We used heat treatment of the base Cu–In–Ga layers in the N_2 inert atmosphere in the presence of selenium and sulfur vapors to synthesize homogeneous films of Cu(In,Ga)(S,Se)$_2$ solid solutions; CdS or In_2S_3 films were then deposited onto the solid-solution films and finally the glass/Mo/*p*-Cu(In,Ga)(S,Se)$_2$/*n*-(In_2S_3, CdS)/*n*-ZnO/Ni–Al were formed. An analysis of the charge-transport mechanism showed that replacement of the barrier layer CdS by In_2S_3 in the obtained TFHPs does not result in significant changes in the electrical properties of these photoelements. Observed broadband photosensitivity of thin-film heterophotoelements and induced photopleochroism are indicative of interference-related bleaching of the obtained structures. It is established that higher quantum efficiency of photoconversion in the heterophotoelements based on Cu(In,Ga)S,Se)$_2$ is attained if thin In_2S_3 films are used as barriers. Thus, as a result of the carried-out physicotechnological study, we established that In_2S_3 films can be introduced into TFHP structure as barriers. This technology can be used in the fabrication of high-efficiency and ecologically safe cadmium-free next-generation TFHPs, while the use of polarization photoelectric spectroscopy can ensure the monitoring of the wide-range blooming of these photoelements.

ACKNOWLEDGMENTS

This study was supported by the Interdisciplinary Scientific and Technological Center (project no. V-1029) and by the program of the Physical Sciences Department of the Russian Academy of Sciences “New Principles of Energy Conversion in Semiconductor Structures.”

REFERENCES

1. N. A. Goryunova, *The Chemistry of Diamond-like Semiconductors* (Leningr. Gos. Univ., Leningrad, 1963; Chapman and Hall, London, 1965).
2. *Copper Indium Diselenide for Photovoltaic Applications*, Ed. by T. J. Coutts, L. L. Kazmerski, and S. Wagner (Elsevier, Amsterdam, 1986).
3. K. Ramanathan, M. A. Contreras, C. L. Perkins, et al., Prog. Photovoltaics: Res. Appl. **11**, 225 (2003).
4. A. Goetzberger, C. Hebling, and H. W. Schock, Mater. Sci. Eng. R **40**, 1 (2003).
5. I. M. Kotschau, M. Turcu, U. Rau, and H. W. Schock, Mater. Res. Soc. Symp. Proc. **668**, H4.5.1 (2001).
6. V. Alberts, J. Titus, and R. W. Birkmire, Thin Solid Films **451–452**, 207 (2004).
7. V. F. Gremenok, E. P. Zaretskaya, V. B. Zalesski, et al., Sol. Energy Mater. Sol. Cells **89**, 129 (2005).

8. I. V. Bodnar', V. A. Polubok, V. F. Gremenok, et al., Fiz. Tekh. Poluprovodn. (St. Petersburg) **41**, 48 (2007) [Semiconductors **41**, 47 (2007)].
9. A. M. Polikanin, O. V. Goncharova, S. A. Sergienya, et al., Zh. Prikl. Spektrosk. **71**, 683 (2004).
10. S. M. Sze, *Physics of Semiconductor Devices*, 2nd ed. (Wiley, New York, 1981; Mir, Moscow, 1984).
11. M. A. Lampert and P. Mark, *Current Injection in Solids* (Academic, New York, 1970; Mir, Moscow, 1973).
12. E. Hernandes, Cryst. Res. Technol. **33**, 285 (1988).
13. V. Yu. Rud', Yu. V. Rud', and H.-W. Schock, Solid State Phenom. **67–68**, 421 (1999).
14. F. P. Kesamanly, V. Yu. Rud', Yu. V. Rud', and G. V. Shok, Fiz. Tekh. Poluprovodn. (St. Petersburg) **33**, 513 (1999) [Semiconductors **33**, 483 (1999)].
15. V. Yu. Rud', Doctoral Dissertation (Ul'yanovsk State Univ., Ul'yanovsk, 2005).
16. E. M. Voronkova, B. N. Grechushnikov, G. I. Distler, and I. P. Petrov, *Optical Materials for Infrared Technology* (Nauka, Moscow, 1965) [in Russian].

Translated by A. Spitsyn